JMEPEG (2010) 19:737–742
DOI: 10.1007/s11665-009-9529-0

1059-9495/$19.00

Magnetic Properties, Microwave Characteristics, and Thermal Stability of the FeCoAlN Films

Jun Zhou, Xudong Zhang, Shu Wang, Hu Wang, and Jiangong Li

(Submitted January 15, 2009; in revised form July 13, 2009)

FeCoAlN films were prepared by reactive radio frequency magnetron co-sputtering technique in an argon and nitrogen mixture atmosphere. The soft magnetic properties, GHz dynamic properties, and magnetic thermal stability of the FeCoAlN films were investigated. The FeCoAlN films deposited at $N_2/(Ar + N_2)$ gas flux percentages larger than 8% have amorphous structure. The $(Fe_{64.8}Co_{35.2})_{96.3}Al_{3.7}N$ film as-deposited at the $N_2/(Ar + N_2)$ gas flux percentage of 9% has good magnetic softness and uniaxial in-plane anisotropy, as demonstrated by the typical hysteresis loops along easy and hard axis. The magnetic thermal stability of the FeCoN films can be obviously improved by introduction of a high Al content. The $(Fe_{64.8}Co_{35.2})_{86.5}Al_{13.5}N$ films annealed at 400 °C for 1 h exhibit good magnetic softness and GHz dynamic properties with a saturation magnetization ($\mu_0 M_s$) of 1.21 T, an easy axis coercive field (H_{ce}) of 8.5 Oe, an anisotropy field (H_k) of 35 Oe, a ferromagnetic resonance frequency (f_r) of 1.89 GHz, and a real part of permeability (μ') of 380. The dynamic characteristics can be described by the theoretical model based on Landau-Lifshitz-Gilbert (L-L-G) equation and eddy current dynamics.

Keywords FeCoAlN thin films, Magnetic property, Thermal stability

1. Introduction

Soft magnetic films with high permeability and ferromagnetic resonance frequency have been studied intensively because of their potential applications in micro-magnetic devices and electromagnetic wave absorption. For these applications, magnetic films should possess high saturation magnetization ($\mu_0 M_s$), high anisotropy field (H_k), high resistivity (ρ), and low coercive field (H_c) to increase work frequency into GHz frequency range (Ref 1). Furthermore, thermal stability is very important to practical applications, especially for the modern semiconductor process in which the soft magnetic materials should withstand the high temperatures above 400 °C (Ref 2). FeXN (X = Ta, Hf, Ti, Al, etc.) films are considered to be promising materials for their excellent soft magnetic properties, high saturation magnetization, and better reliabilities than the FeN films (Ref 3-5). However, the uniaxial anisotropy fields of these films are typically below 20 Oe in the as-deposited states and can be reduced by annealing at temperatures above 150 °C (Ref 6, 7). The recently developed FeCoN films have an in-plane uniaxial anisotropy field usually exceeding 30 Oe and good magnetic softness in as-deposited state (Ref 8-10). However, the FeCoN films suffer from a low magnetic thermal stability (Ref 11). Introduction of proper element can improve the thermal stability of the FeCoN films (Ref 11-13). It is found that the FeCoAlN films with content of Al within 10 to 20% can achieve soft magnetic properties through postannealing in a DC magnetic field (Ref 13). However, the saturation magnetization is reduced evidently because of the high content of Al. Therefore, the relatively low Al content in the FeCoAlN films may get tradeoff between magnetization and thermal stability. The purpose of this work is to study the dependence of the magnetic properties and thermal stability of the FeCoAlN films with relatively low Al content. In this work, the FeCoAlN films are prepared with content of Al (0-13.5%) and the in-plane uniaxial anisotropy is directly induced during the deposition process. The detailed effects of Al content and N_2 flux on soft magnetic properties and GHz dynamic properties are investigated. The temperature effects on dynamic properties are also studied.

Jun Zhou, Xudong Zhang, Shu Wang, Hu Wang, and **Jiangong Li**, MOE Laboratory for Magnetism and Magnetic Materials and Institute of Materials Science and Engineering, Lanzhou University, Lanzhou 730000, China. Contact e-mail: lijg@lzu.edu.cn.

2. Experiments

A series of FeCoAlN films were deposited on glass substrates ($24 \times 24 \times 0.15$ mm^3) by means of the reactive radio frequency (RF) magnetron co-sputtering technique in an $Ar + N_2$ mixture atmosphere. A static magnetic field of about 200 Oe was applied parallel to the substrate surface during deposition to induce an in-plane magnetic anisotropy in the films. An $Fe_{65}Co_{35}$ alloy target of 60 mm in diameter and an Al target of 50 mm in diameter were used as the sputtering targets. The RF power for the $Fe_{65}Co_{35}$ target was kept 90 W; and the RF power of the Al target was changed from 0 to 40 W to adjust the Al content in the films. The base pressure of the sputtering chamber was better than 7×10^{-5} Pa. The Ar gas flux was kept at 25 sccm during sputtering. The nitrogen content in the films was adjusted by changing $N_2/(Ar + N_2)$ gas flux percentages.

The thicknesses of the films were obtained by scanning electron microscope (SEM) observations. The chemical

composition of Fe, Co, and Al in the films was determined by an IRIS Advantage atomic emission spectrometer. The structure of the films was analyzed by x-ray diffraction (XRD) at room temperature on a Rigaku D/Max-2400 x-ray diffractometer with Cu Kα radiation. The static magnetic properties of the thin films were measured by a Lake Shore 7304 vibrating sample magnetometer (VSM) at room temperature. The electrical resistivity was measured at room temperature by a conventional four-point probe method. The complex permeability spectra of the thin films were measured at room temperature in the 0.25 to 4.5 GHz frequency range using shorted microstrip transmission-line perturbation method (Ref 14) with an Agilent PNA E8363B network analyzer.

The thermomagnetic annealing of the films were performed in a vacuum better than 5×10^{-4} Pa. A DC magnetic field of 150 Oe was applied parallel to the film plane during annealing. The direction of this field along the film plane is the same as that used during deposition.

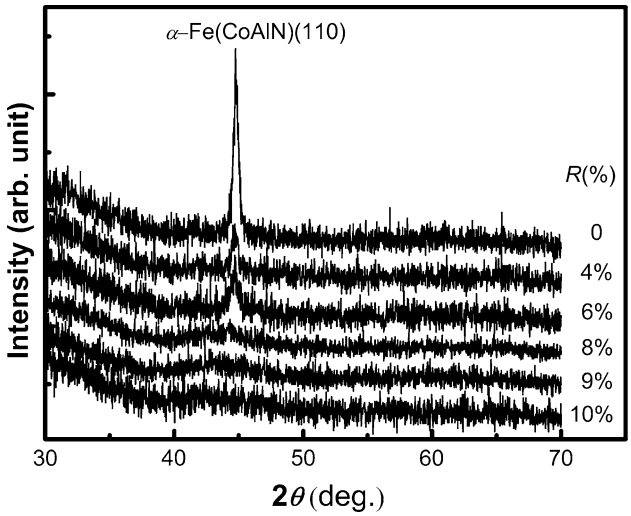

Fig. 1 XRD patterns of the as-deposited $(Fe_{64.8}Co_{35.2})_{93.8}Al_{6.2}N$ films deposited at different $N_2/(Ar + N_2)$ gas flux percentage (R)

3. Results and Discussions

3.1 Structure and Properties of As-Deposited FeCoAlN Films

The FeCoAlN films with different Al contents and $N_2/(Ar + N_2)$ gas flux percentages are prepared and characterized. The Fe:Co atomic ratio in all the thin films is 64.8:35.2. It is assumed reasonably that the nitrogen content in the thin films increases with the increasing $N_2/(Ar + N_2)$ gas flux percentage (Ref 15). Figure 1 shows the XRD patterns of the as-deposited $(Fe_{64.8}Co_{35.2})_{93.8}Al_{6.2}N$ films deposited at different $N_2/(Ar + N_2)$ gas flux percentages. The XRD patterns show only one diffraction peak which is identified as the (110) peak of the α-Fe(CoAlN) phase. The (110) diffraction peak width becomes broader with increasing $N_2/(Ar + N_2)$ gas flux percentage, indicating that the grain size in the films decreases with increasing $N_2/(Ar + N_2)$ gas flux percentage. The average grain sizes of the $(Fe_{64.8}Co_{35.2})_{93.8}Al_{6.2}N$ thin films were estimated from the full width at half maximum (FWHM) of the diffraction peaks using the Scherrer equation. In the process of grain size calculation, the contribution of the apparatus broadening to the FWHM was eliminated. The average grain size of the thin films decreases from 23 nm to less than 9 nm with the $N_2/(Ar + N_2)$ gas flux percentage increasing from 0 to 8%. Meanwhile, the (110) diffraction peak clearly shifts to lower angles with increasing $N_2/(Ar + N_2)$ gas flux percentage, indicating that the lattice expands with increasing nitrogen content. The 2θ value of the (110) diffraction peak of the $(Fe_{64.8}Co_{35.2})_{93.8}Al_{6.2}$ film without N is 44.6°, which is slightly smaller than that of FeCo alloy. It indicates that the introduction of the Al atoms also brings about the lattice expansion of the FeCo alloy because the radius of Al atomic is larger than that of Fe and Co atoms. We can also see clearly from Fig. 1 that the as-deposited films gradually become amorphous in structure when the $N_2/(Ar + N_2)$ gas flux percentage is greater than 8%.

Figure 2 shows saturation magnetization ($\mu_0 M_s$) and resistivity (ρ) of the as-deposited $(Fe_{64.8}Co_{35.2})_{93.8}Al_{6.2}N$ films in variation with the $N_2/(Ar + N_2)$ gas flux percentage. $\mu_0 M_s$ decreases gradually from 2.23 to 1.41 T with the $N_2/(Ar + N_2)$ gas flux percentage increasing from 0 to 12%, as shown in Fig. 2(a). The amorphization and probable formation of the nitride clusters in the films with increasing $N_2/(Ar + N_2)$ gas flux percentage may be the main reason for the decrease in $\mu_0 M_s$ (Ref 4). The variation of resistivity of the $(Fe_{64.8}Co_{35.2})_{93.8}Al_{6.2}N$ films with the $N_2/(Ar + N_2)$ gas flux percentage is shown in Fig. 2(b). The resistivity of the FeCoAl film without nitrogen is 43.7 μΩcm, and the resistivity increases almost linearly from 141.0 to 188.8 μΩcm with the $N_2/(Ar + N_2)$ gas flux percentage increasing from 2 to 12%.

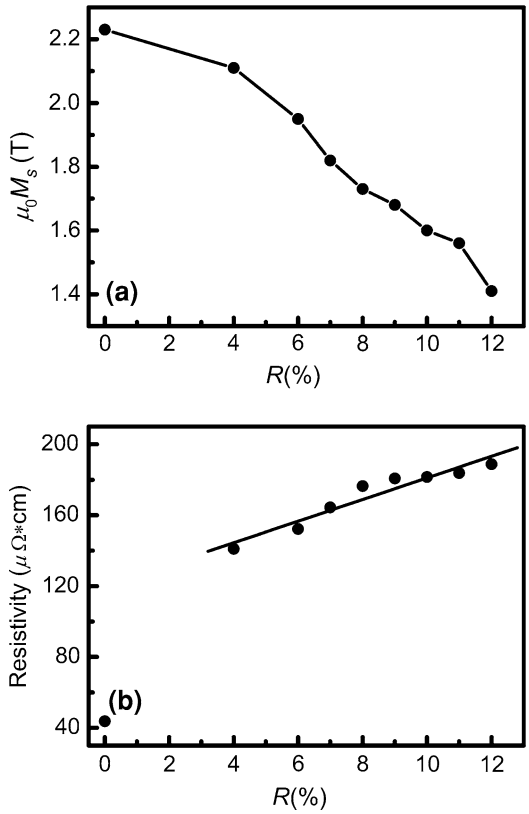

Fig. 2 Saturation magnetization ($\mu_0 M_s$) and resistivity (ρ) of the as-deposited $(Fe_{64.8}Co_{35.2})_{93.8}Al_{6.2}N$ films in variation with $N_2/(Ar + N_2)$ gas flux percentage (R)

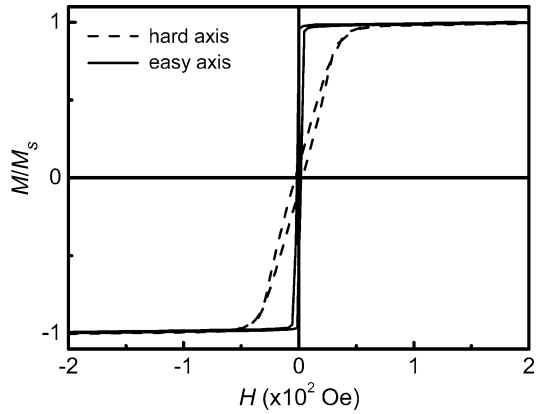

Fig. 3 Hysteresis loops for the as-deposited $(Fe_{64.8}Co_{35.2})_{96.3}Al_{3.7}N$ films deposited at $N_2/(Ar + N_2)$ gas flux percentage of 9%

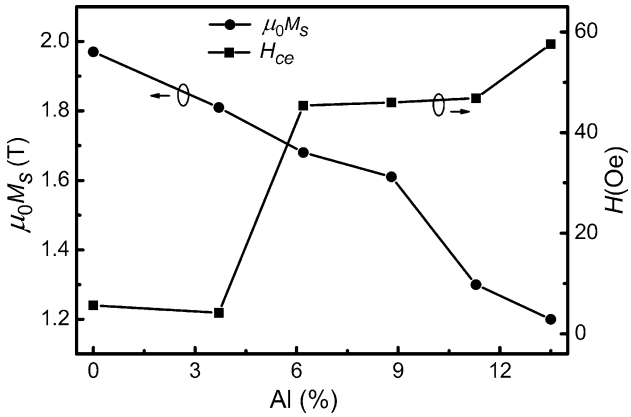

Fig. 4 Saturation magnetization ($\mu_0 M_s$) and the easy axis coercive field (H_{ce}) of the as-deposited $(Fe_{64.8}Co_{35.2})AlN$ films with the different Al contents

The increase in resistivity is likely due to two types of contributions to the scattering of the conduction electrons. One is the grain boundary scattering due to the decrease of the grain size and the volume fraction increase of intergranular phase. The other is the lattice distortion scattering due to the nitrogen interstitial incorporation in the lattice. High resistivity is an important parameter for high frequency application of soft magnetic thin films, as higher resistivity can suppress eddy current loss effectively (Ref 10, 16).

To study the effects of the Al content on the properties of the $(Fe_{64.8}Co_{35.2})AlN$ films, the $N_2/(Ar + N_2)$ gas flux percentage was kept constant at 9% and the Al content was adjusted from 0 to 13.5% by changing the power of the Al target. The XRD patterns (not shown) for the as-deposited films with different Al contents from 0 to 13.5% are almost same as the pattern for the $N_2/(Ar + N_2)$ gas flux percentage of 9% shown in Fig. 1. All the as-deposited films are amorphous. The $(Fe_{64.8}Co_{35.2})_{96.3}Al_{3.7}N$ film deposited at the $N_2/(Ar + N_2)$ gas flux percentage of 9% has good magnetic softness and uniaxial in-plane anisotropy, as demonstrated by the typical hysteresis loops along easy and hard axis shown in Fig. 3. The magnetic exchange interaction in the amorphous or nanocrystalline structure contributes to the soft magnetic properties of the films as described in random anisotropy mode in amorphous or nanocrystalline ferromagnets (Ref 17, 18). Figure 4 shows that $\mu_0 M_s$ decreases from 1.97 to 1.21 T and H_{ce} increases from 5.7 to 57.6 Oe with the Al content increasing from 0 to 13.5%. This attributes to the dilution of magnetization and the increase of stress by introduction of paramagnetic Al.

3.2 The Effects of Al Content on Thermal Stability of the FeCoAlN Films

Good soft magnetic properties require lower magnetic-elastic anisotropy. However, there is usually a high residual stress in the as-deposited FeCoAlN films which cause magneto-elastic anisotropy (Ref 19, 20). Therefore, to release the residual stress and simultaneously test the stability of structure and magnetic properties of the FeCoAlN films, the films were annealed at different temperatures. The hysteresis loops of the FeCoAlN films annealed at different temperatures are shown in Fig. 5. For the specific Al content, H_c decreases initially with increasing annealing temperature because of stress reduction and reaches a minimum at an optimal temperature (T_{opt}). T_{opt} increases gradually with increasing Al content in the FeCoAlN films and are 250 and 400 °C for the films with the Al content of 6.2 and 13.5%, respectively. With increasing annealing temperature (T_a) above T_{opt}, H_c increases obviously. This should attribute to the structure change of the films annealed at T_a above T_{opt}.

To investigate the causations of the magnetic thermal stability described above, the $(Fe_{64.8}Co_{35.2})AlN$ films with Al contents of 6.2 and 13.5% annealed at different temperatures were analyzed by XRD. The XRD patterns of films with 6.2% Al annealed at different temperatures are shown in Fig. 6(a). The as-deposited film with 6.2% Al shows a diffuse peak in the XRD pattern, which is indicative of an amorphous structure. The XRD pattern of the film annealed at 250 °C is similar to that of the as-deposited film. The film annealed at 300 °C shows the obvious diffraction peaks at 43.7° and 44.6° which can be indexed as ε-Fe_3N (111) and α-Fe(CoAlN) (110), respectively. Meanwhile, a diffraction peak for ε-Fe_3N (002) can be found. The XRD patterns of the films with 13.5% Al annealed at different temperatures are shown in Fig. 6(b). The XRD pattern of the as-deposited film with 13.5% Al shows a diffuse peak similar to that of the film with 6.2% Al. The XRD pattern of the film with 13.5% Al annealed at 400 °C shows no obvious change compared to that of the as-deposited film. After annealing at 450 °C, the film shows a strong α-Fe(CoAlN) (110) diffraction peak in the XRD pattern. Accordingly, we can conclude two effects of the Al addition to the FeCoN films. First, the addition of Al facilitates the grain refinement or amorphization of FeCo alloy. Meanwhile, Al can prevent grain growth in the annealing process. Second, the Al addition can suppress effectively the formation of ε-Fe_3N, which has the bad soft magnetic properties, leading to a better thermal stability.

3.3 GHz Dynamic Properties of the FeCoAlN Films

The GHz dynamic properties of the FeCoAlN films were measured with microwave field along the hard axes of the films. The frequency-dependent permeability spectra of the $(Fe_{64.8}Co_{35.2})AlN$ films with Al contents of 6.2 and 13.5% are shown in Fig. 7. The theoretical permeability was described by the model of Landau-Lifshitz-Gilbert (L-L-G) equation coupled with eddy current dynamic magnetization (Ref 21). By fitting the Gilbert damping parameters (α), a good

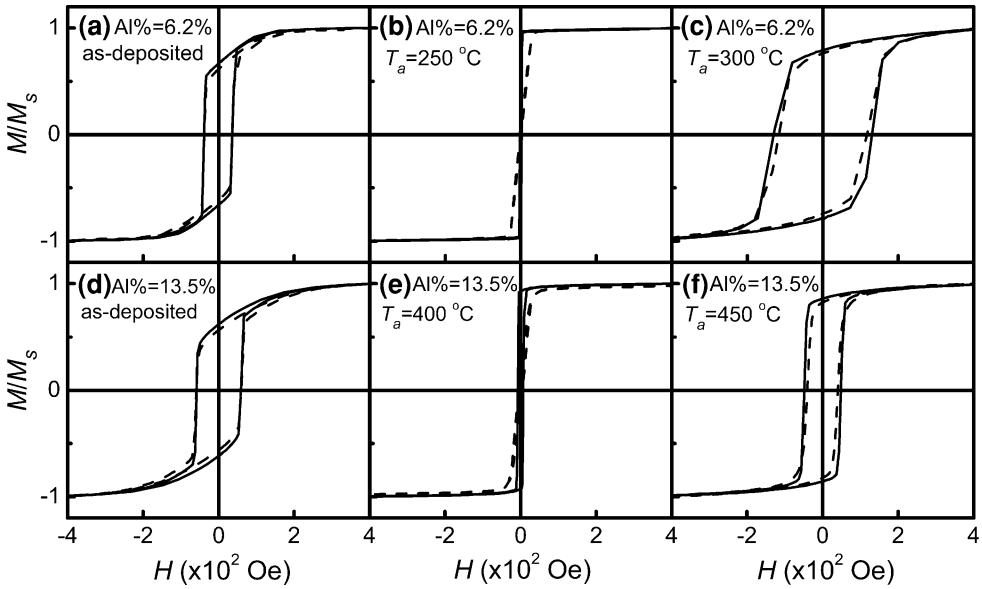

Fig. 5 Hysteresis loops for the $(Fe_{64.8}Co_{35.2})AlN$ films deposited at $N_2/(Ar + N_2)$ gas flux percentage of 9% with different Al contents annealed at different temperatures (T_a). The solid lines are measured along in-plane easy axis and the dashed lines are measured along in-plane hard axis

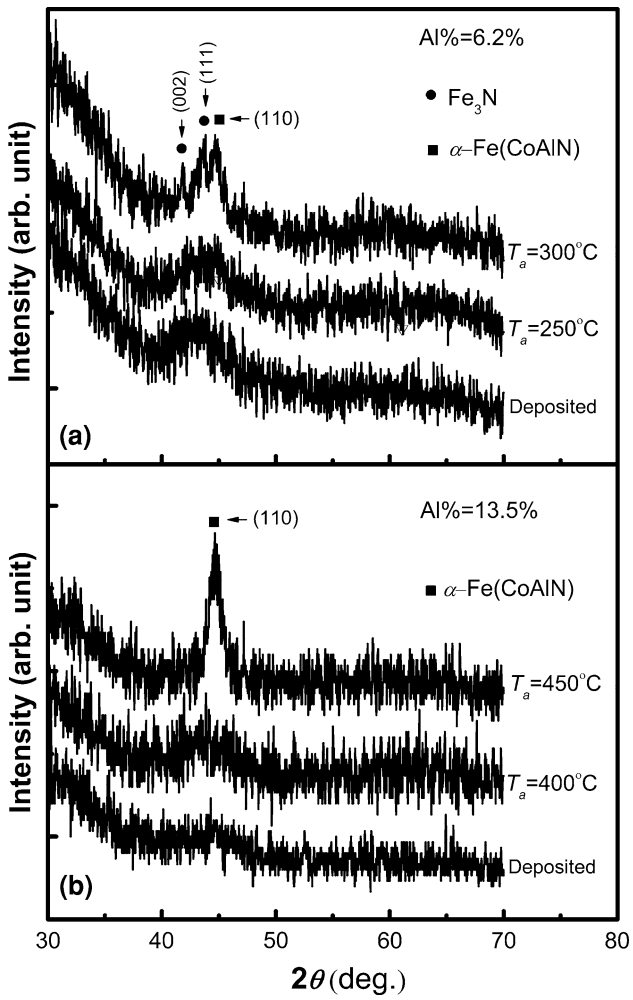

Fig. 6 XRD patterns of the $(Fe_{64.8}Co_{35.2})AlN$ films with the Al contents of 6.2% (a) and 13.5% (b) annealed at different temperatures (T_a)

agreement between the measured and calculated data is obtained, as shown in Fig. 7. The α value of the as-deposited film with Al content of 6.2% is fitted to 0.028, but it decreases to 0.0115 after annealing at 250 °C (Fig. 7a, b). The maximum imaginary part of permeability for the film with an Al content of 6.2% in as-deposited state is 630. The maximum imaginary part of permeability for the film with an Al content of 6.2% annealed at 250 °C is 1350. The permeability spectrum of imaginary part for the as-deposited film with an Al content of 13.5% is relatively flat and has a maximum of about 140. The permeability spectrum of imaginary part for the annealed film with an Al content of 13.5% becomes sharp and has a maximum of 1170 after annealing at 400 °C. The real part of permeability of the film with 13.5% Al annealed at 400 °C is larger than 380 before rolloff. The fitted α value of the film with 13.5% Al annealed at 400 °C is 0.01. This small damping after annealing is consistent with the good soft magnetic properties and uniform magnetization of the film after annealing, as shown in the hysteresis loop (Fig. 5). The reason of these changes may be attributed to the stress relief by annealing. Meanwhile, the annealing at the temperature below T_{opt} cannot lead to the remarkable structure change which can harm the soft magnetic properties, as shown in Fig. 6. Therefore, annealing at a proper temperature can improve the high frequency properties of the FeCoAlN films. And the temperatures that the films could endure are improved obviously with increasing Al content. The measured resonance frequencies are consistent with the calculated from the Kittel's equation $f_r = \gamma(\mu_0 M_s \mu_0 H_k)^{1/2}$, where γ is the gyromagnetic constant (about 2.8 MHz/Oe for the FeCo-based materials). The resonance frequency of the films with Al content of 6.2% annealed at 250 °C and 13.5% annealed at 400 °C are 2.12 and 1.89 GHz, respectively. Although the as-deposited $(Fe_{64.8}Co_{35.2})AlN$ thin films with Al contents of 6.2 and 13.5% do not exhibit good uniform resonance, they exhibit high microwave permeability when annealed at 250 and 400 °C, respectively.

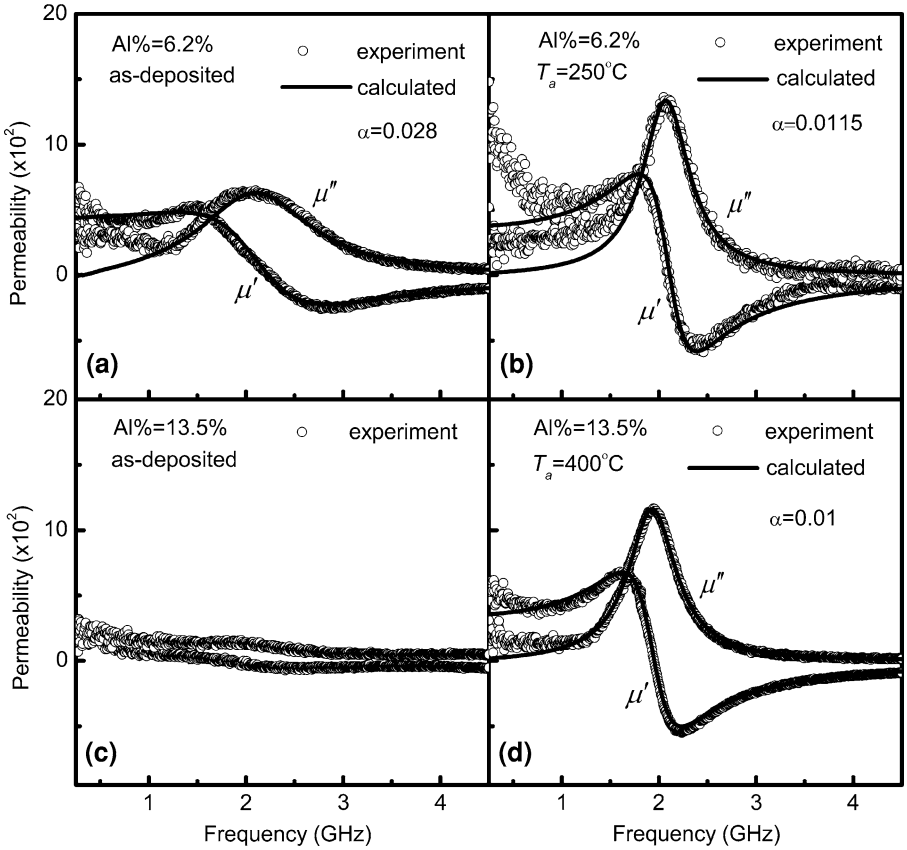

Fig. 7 Permeability spectra of the as-deposited and annealed $(Fe_{64.8}Co_{35.2})$AlN films with the Al contents of 6.2% (a, b) and 13.5% (c, d)

4. Conclusions

The structure of FeCoAlN films deposited at $N_2/(Ar + N_2)$ gas flux percentages of larger than 8% is amorphous. The $(Fe_{64.8}Co_{35.2})_{96.3}Al_{3.7}N$ film as-deposited at the $N_2/(Ar + N_2)$ gas flux percentage of 9% has good magnetic softness and uniaxial in-plane anisotropy, as demonstrated by the typical hysteresis loops along easy and hard axes. The magnetic thermal stability of the FeCoN films can be obviously improved by introduction of a high Al content. The $(Fe_{64.8}Co_{35.2})_{86.5}Al_{13.5}N$ film annealed at 400 °C for 1 h has good soft magnetic properties with a saturation magnetization ($\mu_0 M_s$) of 1.21 T, an easy axis coercive field (H_{ce}) of 8.5 Oe, and an anisotropy field (H_k) of 35 Oe. The ferromagnetic resonance frequency for the $(Fe_{64.8}Co_{35.2})_{86.5}Al_{13.5}N$ film annealed at 400 °C is 1.89 GHz. The real part of permeability of the $(Fe_{64.8}Co_{35.2})_{86.5}Al_{13.5}N$ film annealed at 400 °C is 380 before rolloff and the maximal imaginary part of permeability is 1170. Therefore, the FeCoAlN films of the low content of Al may be a good candidate for high frequency applications.

Acknowledgments

This work was supported by the International S&T Cooperation Program (ISCP) of MOST under 2008DFA50340, the Specialized Research Foundation for the Doctoral Programs of MOE (20070730022), China, and the National Natural Science Foundation of China under 50872046.

References

1. V. Korenivski, GHz Magnetic Film Inductors, *J. Magn. Magn. Mater.*, 2000, **215–216**, p 800–806
2. H.Y. Wang, Y.J. He, Z.W. Ma, E.Y. Jiang, H.S. Huang, and W.H. Mao, High Moment Soft Magnetic FeTiN Thin Films for Recording Head Materials, *J. Appl. Phys.*, 1999, **85**, p 3745–3748
3. D. Peng, K. Sumiyama, and K. Suzuki, Effect of Heat Treatment on the Structure and Magnetic Properties of Fe–N and Fe-Ti-N Alloy Films, *J. Alloys Compd.*, 1997, **255**, p 50–54
4. E.Y. Jiang, D.C. Sun, H. Liu, H.L. Bai, and X.X. Zhang, Structural and Magnetic Properties of Fe–N Gradient Thin Films, *J. Magn. Magn. Mater.*, 1995, **140–144**, p 719–720
5. B. Ma, F.L. Wei, X.X. Liu, C.T. Xiao, and Z. Yang, The Effect of T_a on Structure and Magnetic Properties in Fe–N Films, *Mater. Sci. Eng. B*, 1999, **57**, p 97–101
6. M.K. Minor and J.A. Barnard, Origin and Thermal Stability of H_K in FeTaN Thin Films, *J. Appl. Phys.*, 1999, **85**(8), p 4565–4567
7. Y. Liu and M.H. Kryder, Thermally Stable, Soft FeXN Thin Films, *Appl. Phys. Lett.*, 2000, **77**(3), p 426–428
8. J. Li, X. Zhang, D. Jiao, X. Ni, and S. Wang, Magnetic Properties and High Frequency Characteristics of $(Fe_{81}Co_{19})N$ Thin Films, *Thin Solid Films*, 2008, **516**(10), p 3217–3222
9. N.X. Sun and S.X. Wang, Soft High Saturation Magnetization $(Fe_{0.7}Co_{0.3})_{1-x}N_x$ Thin Films for Inductive Write Heads, *IEEE Trans. Magn.*, 2000, **36**, p 2506–2508
10. Y. Liu, Z.W. Liu, C.Y. Tan, and C.K. Ong, High Frequency Characteristics of FeCoN Thin Films Fabricated by Sputtering at Various $(Ar + N_2)$ Gas Flow Rates, *J. Appl. Phys.*, 2006, **100**(9), p 093912
11. X. Zhang, S. Wang, J. Zhou, J. Li, D. Jiao, and X. Kou, Soft Magnetic Properties, High Frequency Characteristics, and Thermal Stability of Co-Sputtered FeCoTiN Films, *J. Alloys Compd.*, 2009, **474**(1–2), p 273–278

12. K. Seemann, H. Leiste, and V. Bekker, Uniaxial Anisotropy and High-Frequency Permeability of Novel Soft Magnetic FeCoTaN and FeCoAlN Films Field-Annealed at CMOS Temperatures, *J. Magn. Magn. Mater.*, 2004, **283**, p 310–315
13. V. Bekker, K. Seemann, and H. Leiste, Development and Optimisation of Thin Soft Ferromagnetic Fe–Co–Ta–N and Fe–Co–Al–N Films Within-Plane Uniaxial Anisotropy for HF Applications, *J. Magn. Magn. Mater.*, 2006, **296**, p 37–45
14. V. Bekker, K. Seemann, and H. Leiste, A New Strip Line Broad-Band Measurement Evaluation for Determining the Complex Permeability of Thin Ferromagnetic Films, *J. Magn. Magn. Mater.*, 2004, **270**, p 327–332
15. W.C. Chang, D.C. Wu, and J.C. Lin, Effect of Nitrogen Interstitial in α-Fe Crystalline on the Magnetic Soft Properties of FeTaN Thin Films, *J. Appl. Phys.*, 1996, **79**(8), p 5159–5161
16. B. Viala, M.K. Minor, and J.A. Barnard, Microstructure and Magnetism in FeTaN Films Deposited in the Nanocrystalline State, *J. Appl. Phys.*, 1996, **80**(7), p 3941–3956
17. R. Alben, J.J. Becker, and M.C. Chi, Random Anisotropy in Amorphous Ferromagnets, *J. Appl. Phys.*, 1978, **49**(3), p 1653–1658
18. G. Herzer, Grain Structure and Magnetism of Nanocrystalline Ferromagnets, *IEEE Trans. Magn.*, 1989, **25**, p 3327–3329
19. Y. Ma, X. Li, T. Xie, F. Wei, and Z. Yang, A Study of Sputtering Process for Nanocrystalline FeAlN Soft Magnetic Thin Films, *Mater. Sci. Eng. B*, 2003, **103**(3), p 233–240
20. K. Sin and S.X. Wang, Stress and Magnetic Properties in High Moment FeN Thin Films, *J. Appl. Phys.*, 1996, **79**(8), p 5901–5903
21. K. Seemann, H. Leiste, and V. Bekker, New Theoretical Approach to the RF-Dynamics of Soft Magnetic FeTaN Films for CMOS Components, *J. Magn. Magn. Mater.*, 2004, **278**, p 200–207